Food Chemistry: X 20 (2023) 100907

Contents lists available at ScienceDirect

Food Chemistry: X

journal homepage: www.sciencedirect.com/journal/food-chemistry-x

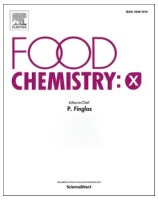

Replacement of fat with highland barley β-glucan in zein-based cheese: Structural, rheological, and textual properties

Lijun Liu [a], Guobao Huang [b], Shuying Li [a], Qifan Meng [a], Fayin Ye [a,c], Jia Chen [a,c], Jian Ming [a,c], Guohua Zhao [a,c], Lin Lei [a,c,*]

[a] College of Food Science, Southwest University, Chongqing 400715, PR China
[b] Guangxi Key Lab of Agricultural Resources Chemistry and Biotechnology, College of Chemistry and Food Science, Yulin Normal University, Yulin, Guangxi 537000, PR China
[c] Chongqing Key Laboratory of Speciality Food Co-Built by Sichuan and Chongqing, Chongqing 400715, PR China

ARTICLE INFO

Keywords:
Plant-based cheese
Zein
Highland barley β-glucan
Stretchability
Melting behavior
Textural properties

ABSTRACT

Nowadays, few plant-based cheese provides satisfactory viscoelastic property like conventional cheese, promoting the application of zein. Our study prepared zein-based cheese containing different concentrations (0–30 %) of highland barley β-glucan (HBG) as a fat replacer. Increased HBG caused smaller and more uniform oil droplets in zein network. SAXS pattern implied R_g decreased from 0.936 nm to 0.567 nm with increased HBG concentration. The stretchability of Cheddar and Violife cheese was 23.69 cm and 6.72 cm, respectively, while that of zein-based cheese added with HBG was 7.76–16.47 cm. The melting behavior of zein-based cheese did not fully mimic Cheddar cheese, but those of HBG5 and HBG10 were more comparable than Violife cheese. Violife cheese lacked hardness and gumminess compared to Cheddar cheese, while more similarities in textural properties were observed between Cheddar and zein-based cheese added with 10 % HBG. Our results provide opportunities in creating meltable low-fat plant-based cheese.

1. Introduction

In recent years, the demand for plant-based products has surged due to increasing consumer concerns regarding human health, environmental sustainability, and animal welfare. While the focus has primarily been on plant-based meat analogues, the market for plant-based dairy analogues, including oat milk, soymilk, tofu, and plant-based cheese, is rapidly expanding (Grossmann & McClements, 2021). For example, the Good Food Institute, a nonprofit organization located at Washington D. C., reported a 3-year dollar sales increase of 85 % for plant-based cheese from 2018 to 2021 (2021 U.S. Retail Sales Data for the Plant-Based Foods Industry, n.d.). However, very few plant-based cheese provides satisfactory sensory and viscoelastic solid-like properties comparable to those of conventional cheese.

One of the key properties of conventional cheese is its ability to flow and stretch above 40 °C, which is attributed to the melting of solid fat and weakening of non-covalent casein network (Lamichhane et al., 2018). Plant-based cheese is a complex colloidal suspension comprised of vegetable oil droplets encapsulated within a network of viscoelastic polysaccharide and/or plant protein (Grossmann & McClements, 2021). To achieve the melting behavior of milk fat in conventional cheese at higher temperatures, manufactures of plant-based cheese often use a high amount of coconut oil and/or palm oil as a solid fat source. However, mimicking the viscoelastic behavior of casein in conventional cheese using polysaccharide and/or plant protein has demonstrated to be quite challenging. Market surveys of plant-based cheese showed a lower meltability than conventional cheese, which was ascribed to the application of non-thermo reversible starch (Nicolás Saraco & Blaxland, 2020). Currently, the functionality of commercial plant-based cheese mainly relies on the contribution of proteins from soy, pea, gluten, potato, cashew nut, and almond. However, plant proteins lead to a gritty taste and varying gelling properties compared to casein micelles. Therefore, the exploration of alternative plant proteins is imperative to address this challenge. One promising trend is the utilization of zein, a hydrophobic prolamin present in maize, for the production of plant-based cheese. A previous study showed mixing a blend of zein, starch, and water at 40 °C resulted in a viscoelastic and extensible gel (Schober et al., 2008). Notably, when zein is dispersed in water, it manifests a

* Corresponding author at: College of Food Science, Southwest University, No. 2 Tiansheng Road, Chongqing 400715, PR China.
E-mail address: leilinsky@swu.edu.cn (L. Lei).

https://doi.org/10.1016/j.fochx.2023.100907
Received 26 February 2023; Received in revised form 12 September 2023; Accepted 27 September 2023
Available online 4 October 2023

rubbery and stretchable texture. This is distinctive from other plant proteins, as it emulates the aggregation behavior observed in casein micelles upon heating (Mattice & Marangoni, 2020a). In contrast to gluten and pea protein-based cheeses, a formulation comprising with 30 % zein, 1.5 % oil, 2.8 % starch, and 0.7 % xanthan displayed comparable rheological, textural, and melt-stretching attributes with Cheddar cheese (Mattice & Marangoni, 2020b).

Although research on the flow-stretching network of zein looks promising for its use in plant-based-cheese, certain limitations still constrain its widespread application. The structural quality of zein network is unsatisfactory in the absence of additives like co-proteins, plasticizers that enhance polymer plasticity, and hydrocolloids. This is primarily due to zein builds protein network only at temperatures above its glass transition temperature (T_g) (Zhang, Xu, et al., 2022). T_g represents the threshold at which the polymer undergoes a transition from a glassy state to a highly elastic state. It signifies the minimum temperature permitting free movement of chain segments within amorphous polymers. The addition of oat bran with a high amount of β-glucan facilitated the creation of a finer zein network, leading to enhanced extensional viscosity of zein-starch system (Andersson et al., 2011). Cereal β-glucan, a soluble linear polymer of β-D-glucose unit linked via (1–3)(1–4) glycosidic bonds distributed abundantly in oats and barley, is regarded as a functional food ingredient due to its hypoglycemic, hypolipidemic, anticancer, and gut microbiota-modulating activities. Furthermore, oat β-glucose is suitable for application in low-fat dairy products owing to its gelling, thickening, stabilizing, and emulsification characteristics (Khorshidian et al., 2018). Several studies have demonstrated the addition of oat β-glucan as a fat-replacer enhances the textural properties of low-fat cheese (Konuklar et al., 2004; Volikakis et al., 2004). In China, since 2014, oat β-glucan has been recognized as a novel food raw material by National Health Commission of the People's Republic of China. This biopolymer can be applied into a myriad of products, including functional foods, beverages, dairy products, and cereal-based meal substitutes. Beyond augmenting the dietary fiber content of these products, it imparts an improved sensory profile. Critically, the incorporation of oat β-glucan facilitates the reduction of both fat and sugar contents. This establishes oat β-glucan as an essential component in the development of products meeting low-sugar, sugar-free, and reduced-sugar criteria.

Highland barley (*Hordeum vulgare L. var. nudum hook. f*), known as hull-less barley or naked barley, is a traditional cereal in the high-altitude areas of Pakistan, Afghanistan, Japan, Nepal, and China. It is notably abundant in β-glucan. But as far as we know, the commercial utilization of highland barley β-glucan (HBG) has not yet received regulatory approval in China, thereby limiting advanced research on its processing within the food industry. Our previous study examined the effects of HBG on linseed oil and soy protein isolate based-oleogels (Ma et al., 2023), demonstrating the potential application of HBG in plant-based analogs. Therefore, the present study aimed to establish a theoretical groundwork for the commercial integration of HBG in low-fat zein-based cheese, with comparison with traditional Cheddar cheese and commercially available plant-based cheese, Violife. The methodology was performed as followes: Firstly, preparation of zein-based cheeses with different HBG contents; secondly, microstructures exploration of these cheeses using confocal laser scanning microscope (CLSM), attenuated total reflectance-Fourier transforms infrared spectroscopy (ATR-FTIR), ultraviolet–visible spectra (UV), and small angle X-ray scattering (SAXS); thirdly, functional properties analysis of these cheeses, with focus on water and oil holding capacity, tensile characteristics, rheological behavior, as well as texture and thermal properties.

2. Materials and methods

2.1. Materials and reagents

HBG (≥85 % purity) with a molecular weight of 2.0×10^5 Da and maize zein (≥95 % purity, containing 75–85 % α-zein, 10 % β-zein, and 5 % γ-zein) with a molecular weight of 3.0×10^4 Da were purchased from Xian Sinuote Biotechnology Co., Ltd., China. Coconut oil, high oleic sunflower oil (≥80 % oleic acid), maize starch, and tapioca starch were obtained from the local market. Swissmooh medium Cheddar cheese and Violife medium cheddar-style plant-based cheese (Cheddar flavor Block), obtained from online supermarket, were used for comparative analysis. From the nutrition label, Cheddar cheese had about 31 % fat, 0 % carbohydrate, and 29 % protein by weight, while Violife plant-based cheese had about 24 % fat, 20 % carbohydrate, and 1.3 % protein by weight. The main ingredients used in Violife plant-based cheese were coconut oil, modified starch, and sunflower kernel grounded. Other chemicals and reagents used were of analytical grade.

2.2. Plant-based cheese formulation

Plant-based cheese samples were prepared using 25 % zein and varying amounts of HBG (0 %, 5 %, 10 %, 15 %, 20 %, 25 %, or 30 % HBG, respectively) following a previous method with modifications (Mattice & Marangoni, 2020b). The contents of starch (a mixture of 33 % maize starch and 67 % tapioca starch by weight) and oil were reduced as the concentration of HBG increased, with the starch-to-oil ratio maintained at 2:1 (compositions and formulations detailed in Supplementary Table 1). To mimic the saturated and unsaturated fat contents in Cheddar cheese, the oil mixture consisted of 25 % high oleic sunflower oil and 75 % coconut oil. All powdered samples (zein, starch, and HBG) were thoroughly mixed, followed by addition of distilled water and oil mixture in an 85 °C water bath. The resulting dough was constantly stirred at 85 °C using a multifunctional mixer (CX-306662, CHIGO, China) at 1500 r/min for 5 min. Then, each sample was placed in a container mold, cooled down to room temperature, and stored at 4 °C for 24 h before analysis.

2.3. CLSM determination

The microstructures were observed by a CLSM (LSM800, Carl Zeiss Jena, Germany) under 200 × magnification described by a method with modifications (Grasso et al., 2021). Prior to fluorescence microscopic examination, each sample was cut into section of 40 μm by a freezing microtome (Leica CM1850, Leica Microsystems Germany). The sample dyed with 50 μL of a mixture of 0.1 mg/mL Nile red in 1,2-propanediol and 0.1 mg/mL Fast Green FCF in water at a ratio of 1:3 under 4 °C for 15 min. Then, the resultant sample was stained with 40 μL of 0.2 wt% Fluorescent Brightener 28 in water for 15 min, washed three times with distilled water, placed on a glass slide, and covered with a glass coverslip before analysis. The Nile Red, Fast Green FCF, and Fluorescent Brightener 28 were excited by 488 nm, 633 nm, and 405 nm Ar laser, respectively. Images were obtained and analyzed with Imaris Viewer (version 9.5.1, Bitplane AG).

2.4. ATR-FTIR determination

Each sample was analyzed using an FTIR spectrometer (Spectrum 100, Perkin-Elmer, USA) equipped with a universal ATR sampling accessory. All measurements were recorded from 4000 cm^{-1} to 600 cm^{-1} with 32 scans and a resolution of 4 cm^{-1} under 25 °C. All spectra were subtracted the background spectrum determined against background of air and analyzed by OMNIC (Thermo, v8.2). Zein and HBG powder were analyzed for comparison.

2.5. UV spectra determination

Each sample was analyzed using UV spectrophotometer (TU-1950, Persee Instrument, China). The protein concentration was fixed at 22.7 μmol/L. The scanning ranged from 190 nm to 600 nm. Baseline was corrected with 80 % ethanol solution (v/v) before scanning. Zein

powder was analyzed for comparison.

2.6. SAXS determination

The SAXS analysis was performed using the 1W2A SAXS station in the Beijing Synchrotron Radiation Facility. The electron energy was 2.5 GeV and the beam current was 180 mA. The sample-detector distance was 1718 mm and the wavelength of synchrotron radiation was 0.154 nm using a Mar 165 CCD detector at 25 °C. The exposure time was 100 s. The obtained 2D diffraction images were analyzed by Fit2D software. Guinier analyses were calculated from the scattering patterns using functions of BioXTAS RAW. The resultant Guinier plot, instrumental in determining R_g, was shown in Supplementary Fig. 2. The scattering vector was defined by Eq. (1) (Suzuki et al., 1997), where 2θ was the scattering angle and λ was the X-ray wavelength.

$$q = (4\pi/\lambda)\sin(2\theta) \quad (1)$$

The lamellar and fractal structures of each sample were described as fractal dimension and the radius of gyration (R_g). The scattering patter from a fractal object obeyed a power law by Eq. (2) (Suzuki et al., 1997), where I indicated scattering intensity and q indicated the scattering vector.

$$I \propto q\ \alpha \quad (2)$$

In general, the fractal characteristics were indicated by exponent α, the slope of the regression line of the double logarithmic SAXS curve. $-4 < \alpha <$ -3, defined as surface fractal, indicated the scattering could be characterized as reflection from the surface or interface. $-3 < \alpha <$ -1, defined as mass fractal, indicated the density profile of the scattering object had a self-similar nature. The surface fractal dimension D_s and the mass fractal dimension D_m could be obtained by Eq. (3) and Eq. (4), respectively.

$$D_S = 6 + \alpha \quad (3)$$

$$D_m = -\alpha \quad (4)$$

R_g indicated the average distance of polymer from its center of mass calculated by Eq. (5) (Chalal et al., 2010), where I_g (0) was the zero angle scattering intensity.

$$\mathrm{Ig(q)} = \mathrm{Ig(0)exp(-q2Rg2/3)} \quad (5)$$

2.7. Analysis of moisture, color, and water-holding capacity (WHC)

The moisture content of each sample was analyzed according to the Chinese National Standard (GB 5009.3–2016). Lightness (L^*), redness (a^*), and yellowness (b^*) color values were determined using Ultrascan PRO Hunterlab colorimeter (Hunter Lab, Reston, USA). WHC was analyzed using centrifuge according to a previous method with modifications. 2 g sample was added into a 10 mL centrifuge tube and centrifuged 10,000 g for 15 min at 4 °C. Water expelled after centrifugation was measured and WHC was calculated as Eq. (6)

$$WHC(\%) = \left[1 - \frac{m_3}{(m_2 - m_1) \times x}\right] \times 100\% \quad (6)$$

m_1, the mass of the empty centrifuge tube (g); m_2, the mass of the centrifuge tube and the sample before centrifugation (g); m_3, the mass of the centrifuge tube and the sample after the water was removed; x stands for the content of water in the sample.

2.8. Analysis of stretch and free oil released characteristics

Stretchability was determined by a previous method with modifications (Lilbæk et al., 2006). A square sample with 4 cm width (~1 cm in thickness) was cut from the inside of cheese and placed in a glass petri dish under room temperature for 30 min. and then heated in a water bath under 90 °C for 10 min. The sample was subsequently heated in a water bath at 90 °C for 10 min before being stretched by fixing one end and lifting the other using forceps. The rupture distance (cm) was measured to assess the stretchability behavior.

Free oil-release was determined by a previous method with modifications (Moghiseh et al., 2021). A sample with 30 mm in diameter and 5 mm in thickness was cut from the interior of the cheese and placed at room temperature for 30 min. Then, each sample was put on a glass petri dish with filter paper, heated in an oven at 90 °C for 20 min, and cooled at room temperature for 60 min before photographed. The diameter (cm) of the free oil on the filter paper was analyzed using Image J software (National Institutes Health, Bethesda, MD, USA) to evaluate the free oil-release.

2.9. Rheological determination

The rheology was determined by the methods with slight modifications (Mattice & Marangoni, 2020b) using a rotational rheometer (DHR-2, TA Instruments, USA). Briefly, 5.0 g sample was put on the lower plate and compressed to a thickness of 2500 μm by with a parallel plate with 40 mm diameter. Temperature sweeps were performed from 4 °C to 100 °C under shear strain $\gamma = 0.01$ % and angular frequency $\omega = 3$ rad/s. Strain sweeps test were performed at strain amplitude ranging from $\gamma =$ 0.01 % to $\gamma = 1000$ % at $\omega = 3$ rad/s under 60 °C.

2.10. Differential scanning calorimetry (DSC)

Thermograms of all samples were analyzed by a DSC 4000 calorimeter (Perkin Elmer Ltd, Waltham, US). 10 mg sample was packed into a standard aluminum pan and heated from 0 °C to 60 °C at a rate of 5 ∘C/min. An empty pan was used as reference. Data was processed using Pyris software (Perkin-Elmer, Shelton, CT, USA).

2.11. Texture profile analysis

Texture analysis was performed by a Texture Analyzer (TA. XT Plus, Stable Micro System, UK) using a previous method with slight modifications (Mattice & Marangoni, 2020b) at 4 °C, 37 °C and 60 °C, respectively. Each sample was cut into a square with 4 cm width (~1 cm in thickness) and compressed to 75 % of their original height. Measurements were performed using a P/36R cylinder probe (30 mm diameter) under a constant speed of 1.5 mm/s.

2.12. Statistical analysis

Data were expressed as means ± standard deviation. Six measurements were performed for texture analysis and all other tests were measured in triplicate. Means were analyzed by one-way analysis of variance (ANOVA) followed by Turkey's multiple-range test using GraphPad Prism 8 (GraphPad Software Inc.; San Diego, CA, USA). The significance was set at $p < 0.05$.

3. Result and discussion

3.1. Characterization of zein-based cheese

3.1.1. The visual appearance of surface and cross-section of zein-based cheese

Fig. 1A illustrates the surface and Supplementary Fig. 1 shows cross-section views of Cheddar cheese, Violife cheese, and zein-based cheese. Unlike Cheddar cheese (Fig. 1A), the free oil in Violife cheese was not fully emulsified by starch, resulting in oil separation (Ye et al., 2009). The surface of zein-based cheese without HBG (HBG0) appeared greasy, rough, and yellowish. However, with the addition of HBG at concentrations of 5–15 %, the surface of zein-based cheese became drier and smoother. On the contrary, HBG addition above 20 % caused brittle

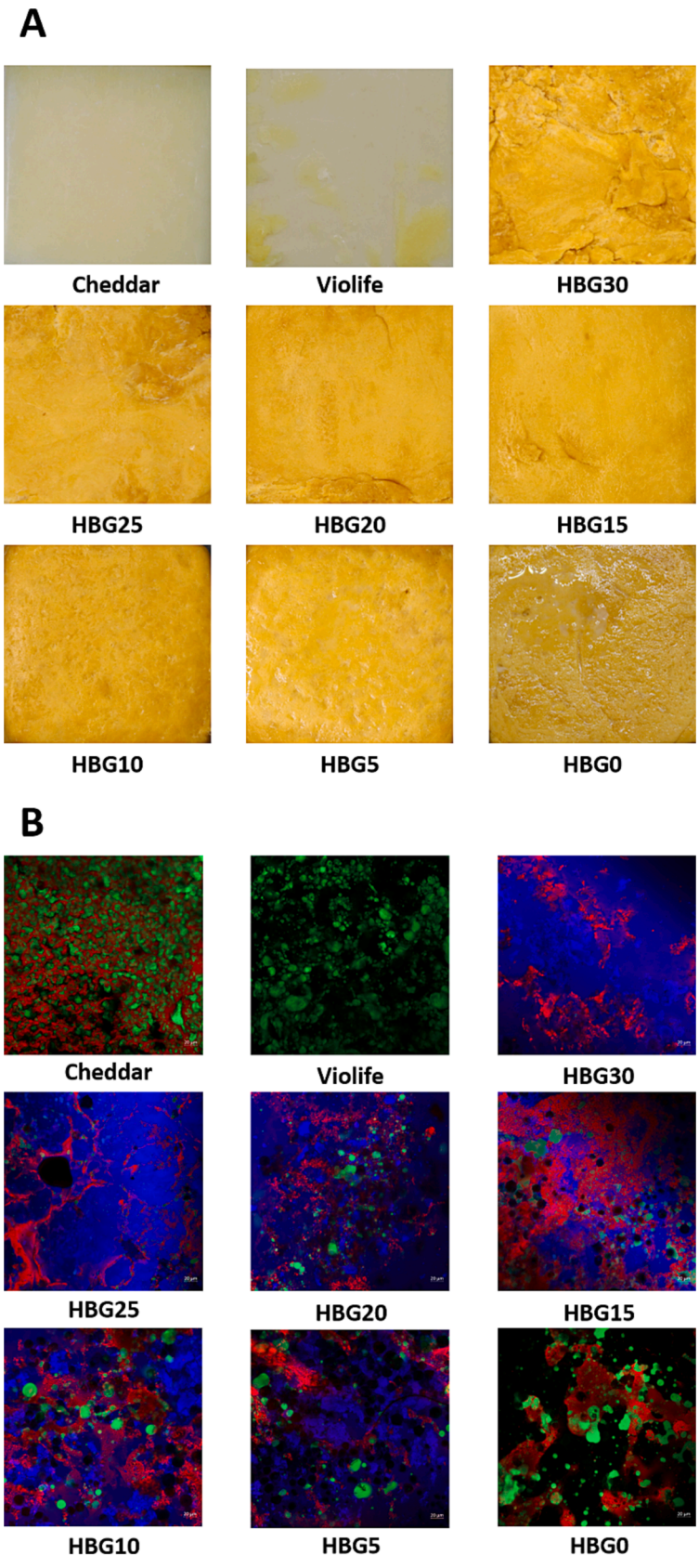

(caption on next page)

Fig. 1. Visual appearance of surface (A) and microstructures(B) of Cheddar, Violife, and zein-based cheeses with different concentrations of highland barley β-glucan. HBG0, zein-based cheese without highland barley β-glucan; HBG5, zein-based cheese added with 5 % highland barley β-glucan; HBG10, zein-based cheese added with 10 % highland barley β-glucan; HBG15, zein-based cheese added with 15 % highland barley β-glucan; HBG20, zein-based cheese added with 20 % highland barley β-glucan; HBG25, zein-based cheese added with 25 % highland barley β-glucan; HBG30, zein-based cheese added with 30 % highland barley β-glucan. The laser scanning confocal microscope images (200 ×) of cheeses (oil dyed in green, protein dyed in red, and HBG dyed in blue). (For interpretation of the references to color in this figure legend, the reader is referred to the web version of this article.)

texture and non-homogeneous surface due to reduced oil content (Fig. 1A). The cross-sectional appearance of zein-based cheese showed a similar trend as HBG concentrations increased (Supplementary Fig. 1).

3.1.2. The morphology of zein-based cheese

Fig. 1B depicts the CLSM images of all samples, with fluorescent brightener (HBG), Fast Green FCF (zein), and Nile red (oil) showing blue, red, and green, respectively. Cheddar cheese presented a compact structure, with non-spherical shaped coalesced pockets/pools of fat globules evenly dispersed in a continuous protein matrix. The shape of milk fat globules in Cheddar cheese was resulted by the shearing during milk handling and coalescence of fat globules during cheese manufacture (Grasso et al., 2021). In comparison, Violife cheese had larger and spherical oil droplets within the starch matrix (black area) (Grasso et al., 2021; Ye et al., 2009). The microstructures formed by zein, HBG, and starch were different from Cheddar and Violife cheeses. Without HBG (HBG0), the entire system contained the largest, aggregated, and unevenly distributed oil droplets. As the concentration of HBG increased while the oil content decreased (HBG5-HBG30), fewer but smaller and more compact oil droplets dispersed in the zein-HBG network. HBG, a non-surface-active polysaccharide, acts as a thickener to ensure saturation of the oil–water interface. Oat β-glucan caused smaller and more uniform fat globules and more compact matrix in processed cheese by inducing increased viscosity and stability (Florczuk et al., 2023). Moreover, at the concentration of 25 % and 30 %, respectively, HBG was no longer distributed in strands but as large clusters. HBG strands or clusters seemed to link together and disrupt the continuous zein matrix, which were also found in rennet–casein-based model processed cheese containing maize starch (Ye et al., 2009).

3.1.3. FTIR spectra

The FTIR spectra of all samples are presented in Fig. 2A. Broad peaks at around 3200–3300 cm^{-1} in the spectra derived from O—H stretching in hydroxyl groups. Cheddar cheese showed typical FTIR spectra in the range of 2917–900 cm^{-1}, including CH stretching of fatty acids at 2917–2852 cm^{-1}, C═O of acids and esters at 1780–1720 cm^{-1}, amide I and amide II of proteins at 1710–1580 cm^{-1}, esters and aliphatic chains of fatty acids at 1570–1220 cm^{-1}, and C═O and C—O stretching of acids at 1210–950 cm^{-} (Subramanian et al., 2011). For Violife cheese, due to the lack of protein and the addition of starch, the protein absorption

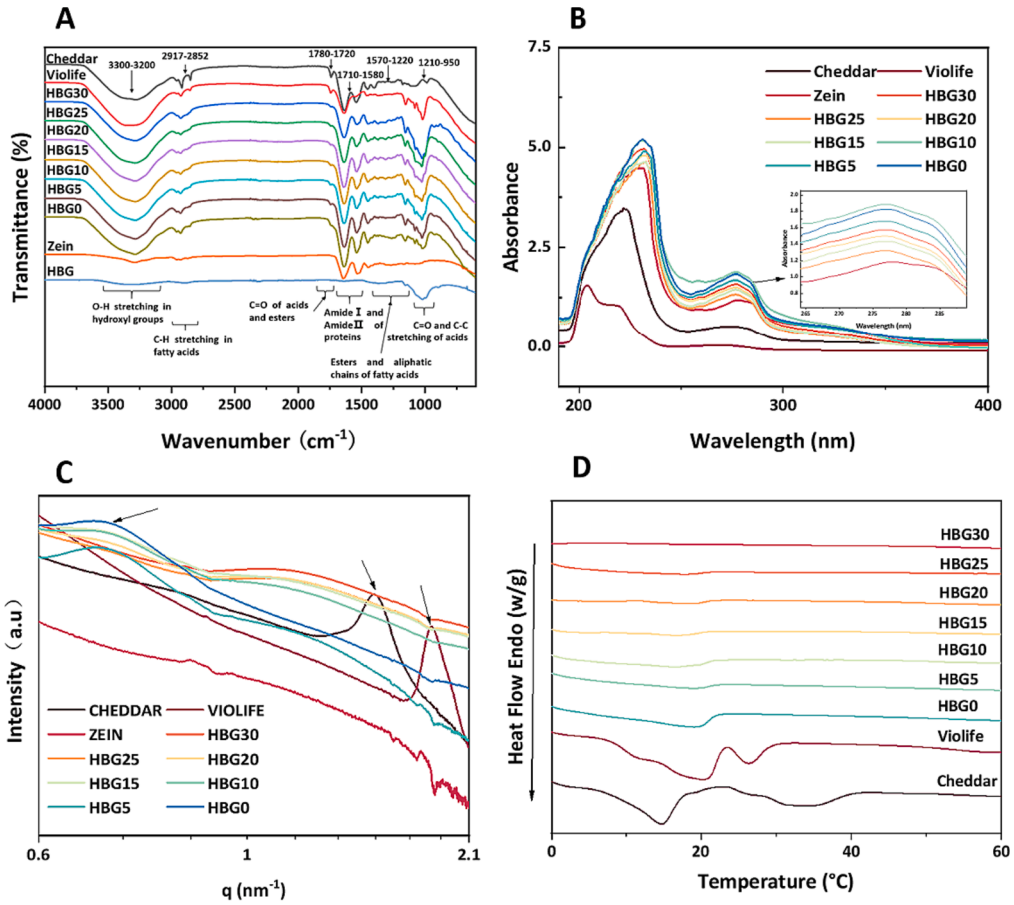

Fig. 2. Fourier transform infrared spectroscopy (A), UV–Vis (B), small angle X-ray scattering (C), and differential scanning calorimetry curves (D) of Cheddar, Violife, and zein-based cheeses with different concentrations of highland barley β-glucan. HBG0, zein-based cheese without highland barley β-glucan; HBG5, zein-based cheese added with 5% highland barley β-glucan; HBG10, zein-based cheese added with 10% highland barley β-glucan; HBG15, zein-based cheese added with 15% highland barley β-glucan; HBG20, zein-based cheese added with 20% highland barley β-glucan; HBG25, zein-based cheese added with 25% highland barley β-glucan; HBG30, zein-based cheese added with 30% highland barley β-glucan.

bands (1710–1580 cm^{-1}) disappeared, while the intensity of peaks at 1210–950 cm^{-1} (the C═O and C—O stretching of acids) became stronger. Zein showed typical spectra of protein at around 1710–1580 cm^{-1}. HBG exhibited typical spectra of polysaccharides at around 3200–3300 cm^{-1}, 1029 cm^{-1}, and 894 cm^{-1}, which corresponded to the stretching vibrations of O—H, C—O—C, and β-linked glycosidic bond, respectively (Bai et al., 2021). The addition of HBG to zein caused broader peaks at around 3200–3300 cm^{-1}, demonstrating the formation of a 3D network mainly through the stretching intramolecular or intermolecular hydrogen bonding in the complexes (Jin, 2020). No significant differences were observed among FTIR spectra of zein-based cheese with different HBG concentrations.

3.1.4. Uv–vis spectra

The conformational changes of zein-HBG complex are characterized by the near UV-region (200–400 nm) (Fig. 2B). Cheddar cheese presented weak absorption at around 280 nm, the typical UV spectrum of casein (Kong et al., 2021). In contrast, this absorption band disappeared in Violife cheese. Zein also exhibited a typical UV absorption at around 280 nm due to vibrations of tyrosine and tryptophan residues (Sun et al., 2016). The addition of HBG to zein made a red-shift of the absorption and an increase in the peak intensity at 280 nm (HBG5-HBG30), indicating a conformational change of zein. This might be owing to the exposure of more tyrosine heterocyclic residues or the formation of hydrogen bonds with tyrosine phenolic moieties when complexation with HBG (Chen et al., 2020).

3.1.5. Lamellar and fractal structure

The double logarithmic SAXS patterns of all samples are presented in Fig. 2C. Cheddar cheese presented a main peak at $q = 1.597$ nm^{-1}. It indicated milk fat crystalline phase showed a lamellar thickness corresponding to the length of two aliphatic chains (Arita-Merino et al., 2022). A scattering peak at $q = 1.887$ nm^{-1} was observed in Violife cheese, indicating the lamellar liquid crystal of coconut oil (Arifin et al., 2021).No obvious scattering peaks were observed in zein powder over the small-angle range, indicating molecular aggregates of zein powder did not have long-range periodicity (Wang et al., 2005). However, scattering peaks of zein-based cheese containing 0–30 % HBG lied at 0.603–0.895 nm^{-1}, indicating the semi-crystalline lamellar structure of maize starch and tapioca starch (Zhang, Junejo, et al., 2022).

Table 1 presents SAXS parameters of all samples. Cheddar and Violife cheeses had surface fractal due to $\alpha < -3$. The larger surface fractal dimension (D_s) of Cheddar cheese indicated a higher degree of surface irregularity of the scattering objects (Suzuki et al., 1997). α of zein and zein-based cheese containing 0–30 % HBG varied from −3 to −1, which could be defined as "mass fractal". The larger mass fractal dimension (D_m) of HBG5 and HBG10 indicated a higher compactness of the scattering object mass (Suzuki et al., 1997). Scattering objects with surface fractal structure were more compact than those with mass fractal structure (Liu et al., 2019), which were in accordance with our CLSM images (Fig. 1B). Cross-linking played a critical role in R_g. Accompanied by higher concentrations of HBG, R_g decreased from 0.936 nm^{-1} to 0.567 nm^{-1} (Table 1). This might be because HBG crosslinker restricted chain extensions within the plant-based cheese constructed by starch, zein, and water molecules (Qiao et al., 2019).

Table 1
Small X-ray scattering parameters of Cheddar, Violife, and zein-based cheeses with different concentration of highland barley β-glucan.

Samples	α	R_g (nm)	D_s(nm)	D_m(nm)
Cheddar	−3.272	0.657	2.729	——
Violife	−3.203	0.706	2.797	——
Zein	−2.097	0.780	——	2.097
HBG30	−1.791	0.567	——	1.791
HBG25	−1.924	0.581	——	1.924
HBG20	−2.046	0.590	——	2.046
HBG15	−2.253	0.602	——	2.253
HBG10	−2.633	0.605	——	2.633
HBG5	−2.767	0.958	——	2.767
HBG0	−2.228	0.936	——	2.228

HBG0, zein-based cheese without highland barley β-glucan; HBG5, zein-based cheese added with 5% highland barley β-glucan; HBG10, zein-based cheese added with 10% highland barley β-glucan; HBG15, zein-based cheese added with 15% highland barley β-glucan; HBG20, zein-based cheese added with 20% highland barley β-glucan; HBG25, zein-based cheese added with 25% highland barley β-glucan; HBG30, zein-based cheese added with 30% highland barley β-glucan.

3.2. Functional properties of zein-based cheese

3.2.1. Moisture, color, and WHC

Table 2 showed Violife cheese had the highest moisture content while Cheddar cheese had the lowest. The moisture contents of zein-based cheese reduced with increasing HBG concentrations. The color was affected by oil types (*e.g.*, milk fat *v.s.* vegetable oils), colorants (*e.g.*, β-carotene), and the manufacturing process. Violife cheese had the highest L^* value of all samples because it had the smoothest, softest, and brightest surface. Compared to Cheddar and other zein-based cheeses, HBG0 and HBG5 had greasier surfaces and showed greater L^* values (Table 2). b^* value, indicating the degree of yellowness to blueness, decreased from 43.85 in HBG0 to 25.87 in HBG30 as the yellowish sunflower oil content decreased. Addition of β-carotene made Violife cheese have a higher b^* value than that of Cheddar cheese (Table 2) (Grasso et al., 2021). The addition of HBG formed a more ordered structure via hydrogen bonding (Fig. 1B), which restricted water migration and resulted in an increased water-holding capacity of zein-based cheese compared with HBG0 (Table 2) (Y. Zhang et al., 2019).

3.2.2. Stretchability and free oil-release

Table 2 shows changes of stretchability and free-oil release of all samples. Stretchability, one of important properties of cheese products, refers to the ability of casein network to maintain its integrity without breaking when sustained stress applied to the cheese at higher temperatures. Stretchability of the melted Cheddar cheese (23.69 cm) was significantly higher than that of the melted Violife (6.72 cm) or zein-based cheeses (9.22–16.47 cm). Stretchability was affected by ingredients of cheese formulations, especially proteins. Zein has a glass transition temperature (T_g) of 139 °C in a dry state, but the presence of water plasticizes the protein. This can create rubbery stretchable mass at temperatures under T_g (McClements & Grossmann, 2022). Mattice and Marangoni reported zein was critical to make plant-based cheese with similar textural properties as Cheddar cheese (Mattice & Marangoni, 2020b). The observed stretchability of HBG10 (16.47 cm) added to the list of its cheese-like characteristics, demonstrating the promising application of zein/HBG mixed system in plant-based cheese. However, the stretchability of zein-based cheese added with 15–30 % HBG started to decrease from 14.48 cm to 7.76 cm, indicating the viscoelastic zein network became brittle with further increased amount of HBG. Free oil-release was nil in HBG30 because of the absence of oil, but highest in Cheddar cheese. The weakening of casein network caused fat droplets to coalesce and flow to the surface upon heating. During baking, some oiling-release from cheese was desirable. Because free oil rapidly formed a surface-oil layer on melted cheese, which restricted the dehydration and associated defects (Rudan & Barbano, 1998). Our result was in agreement with findings of Dai et al (Dai et al., 2019)who reported increasing fat concentrations were observed with remarkedly higher free oil-release in conventional cheese.

3.2.3. Oscillatory temperature sweeps

The melting behaviors of cheese samples were analyzed by temperature sweeps (Fig. 3A-D). Generally, G' and G'' represent the softening and flow ability of conventional cheese, an effect caused by 1) the liquefaction of the fat phase and 2) contraction and shrinkage of *para-*

Table 2
Moisture, color, water-holding capacity, stretchability, meltability, and free oil-release of Cheddar, Violife, and zein-based cheeses with different concentrations of highland barley β-glucan.

	Cheddar	Violife	HBG30	HBG25	HBG20	HBG15	HBG10	HBG5	HBG0
Moisture (%)	32.46 ± 0.90a	48.03 ± 0.88 g	39.26 ± 0.95b	40.08 ± 0.61bc	40.36 ± 0.71bcd	41.24 ± 0.46 cd	42.07 ± 0.61de	43.22 ± 0.30ef	44.41 ± 0.12f
L*	69.02 ± 1.42c	85.06 ± 0.45f	69.39 ± 1.10c	64.29 ± 0.45a	65.15 ± 0.60a	66.94 ± 0.52b	69.70 ± 0.28c	73.92 ± 0.67d	76.57 ± 0.45e
a*	−1.16 ± 0.32a	3.87 ± 0.04b	6.24 ± 0.36c	9.05 ± 0.21e	9.06 ± 0.41e	8.03 ± 0.23d	7.46 ± 0.27d	6.62 ± 0.28c	5.96 ± 0.21c
b*	22.28 ± 2.69a	32.11 ± 0.36c	25.87 ± 1.64b	34.10 ± 0.69 cd	38.93 ± 1.42ef	36.99 ± 1.07de	39.18 ± 0.75ef	41.50 ± 0.84 fg	43.85 ± 1.39 g
Water-holding capacity (%)	99.75 ± 0.00bc	99.55 ± 0.46b	99.93 ± 0.02c	99.85 ± 0.12bc	99.71 ± 0.30bc	99.93 ± 0.01c	99.31 ± 0.01bc	98.95 ± 0.28b	93.91 ± 0.35a
Stretchability (cm)	23.69 ± 0.21 h	6.72 ± 0.07a	7.76 ± 0.01b	13.83 ± 0.02e	13.95 ± 0.12e	14.48 ± 0.07f	16.47 ± 0.05 g	11.15 ± 0.11d	9.22 ± 0.18c
Free oil-release (cm)	4.60 ± 0.58c	1.64 ± 0.44ab	——	1.36 ± 0.29a	1.42 ± 0.24ab	1.68 ± 0.28ab	1.69 ± 0.41ab	2.01 ± 0.65ab	2.21 ± 0.40b

HBG0, zein-based cheese without highland barley β-glucan; HBG5, zein-based cheese added with 5 % highland barley β-glucan; HBG10, zein-based cheese added with 10 % highland barley β-glucan; HBG15, zein-based cheese added with 15 % highland barley β-glucan; HBG20, zein-based cheese added with 20 % highland barley β-glucan; HBG25, zein-based cheese added with 25 % highland barley β-glucan; HBG30, zein-based cheese added with 30 % highland barley β-glucan. Different letters in the same row indicate significant differences ($p < 0.05$).

casein network between 60 °C and 90 °C (Fox et al., 2017). The viscoelastic properties could differentiate the melting behavior of Cheddar cheese at varied ages, protein and fat contents, moisture, emulsifying salts, etc. A crossover temperature between *G'* and *G''* was observed at around 60 °C in Cheddar cheese (Fig. 3A), suggesting the transition from a viscoelastic solid to a viscoelastic liquid (Fox et al., 2017). Instead, Violife cheese showed a gentler slope of *G'* and *G''* and closely approaching each other after 70 °C (Fig. 3A). This was probably because the high content of starch in Violife cheese kept high elasticity and delayed the meltability. (Grasso et al., 2021; Mattice & Marangoni, 2020b; Ye et al., 2009). Heating softened zein-based cheeses by weakening the non-covalent bonds, however HBG0 exhibited a different melting profile with increasing temperature (Fig. 3A). Specifically, zein network of HBG0 displayed a greater viscosity within the range of 23–72 °C. Curves of *G'* and *G''* in HBG0 approached each other and then *G'* values slightly higher than *G''* values (Mattice & Marangoni, 2020a). HBG5 and HBG10 exhibited more noticeable melting during heating, because their slopes of *G'* and *G''* values decreased more abruptly (Fig. u.3B) (Mattice & Marangoni, 2020b). While samples containing 15–30 % zein maintained more elastic and slightly softened, as evidence by the gradual slope of *G'* and *G''* with elevated temperature (Fig. 3C-D). Notably, G' of HBG0 and HBG5 firstly declined and then increased (Fig. 3A & B). The ascending trend was likely due to the enhanced hydrophobic interactions and polymerization of zein induced by high temperature (Mattice & Marangoni, 2020a; Zhang, Gao et al., 2022). This effect on zein-HBG network, however, was diminished as the HBG concentration increased from 10 to 30 % (Fig. 3 B-D). The melting curves of zein-based cheese did not fully mimic that of Cheddar cheese, but those of HBG5 and HBG10 were notably more comparable than Violife cheese.

3.2.4. Oscillatory amplitude sweeps

Amplitude sweeps were performed at 60 °C when Cheddar cheese was completely melted. Cheddar and zein-based cheese supplemented with 0–10 % HBG were analyzed because of similarities among them observed in temperature sweeps. For all samples, *G'* values higher than *G''* within the linear viscoelastic region (LVR) indicated the existence of gel-like properties at low strain rates (Fig. 3E & F). Cheddar and zein-based cheese samples presented more similar behavior in LVR. Violife cheese behaved a greater elasticity because of the high starch content (Mattice & Marangoni, 2020b). Cheddar cheese reached the crossover point of *G'* and *G''* (~2.6 %) earlier than Violife cheese (~139.4 %), HBG0 (~16.9 %), HBG5(~10.5 %), and HBG10 (~3.2 %). Both *G'* and *G''* values of zein-based cheese within LVR were markedly higher than those of Cheddar cheese, indicating the need for plasticization of zein to improve the flowability.

To assess the brittleness of all samples, shear stress values were plotted against shear strain (Fig. 3G). Brittleness refers to the material's structure destroyed or irreversibly damaged when the maximum stress value is achieved. Both Cheddar and Violife cheeses exhibited increased stress with increased strain, indicating their structures could maintain integrity. However, Cheddar cheese was much softer (lower G') compared with Violife cheese. Mattice and Marangoni found Cheddar cheese showed weak and brittle properties at 50 °C (Mattice & Marangoni, 2020b, 2020a). In our study, this peak transformed into a plateau at 60 °C, suggesting that Cheddar cheese necked after yielding before failing at higher temperatures (Muliawan, 2008). HBG0 showed a typical profile of "soft solid" materials due to the presence of zein (Erni et al., 2007). However, the addition of HBG into zein-based cheese samples decreased the maximum shear stress, which occurred at nearly the same shear strain in spite of HBG concentrations.

3.2.5. Thermal property

The thermal properties of all samples are shown in Fig. 2D. Cheddar cheese presented a typical thermogram with the first peak at ~ 14 °C and the second at ~ 32 °C, corresponding to the melting of low and medium melting fractions and high melting fraction of milk fat, respectively (Grasso et al., 2021). Violife cheese and zein-based cheese without HBG (HBG0) presented broad endotherms at ~ 20 °C, corresponding to the melting of coconut oil. However, no obvious endothermic peak was observed due to the interaction between zein and HBG.

3.2.6. Texture qualities

The effects of HBG on hardness, springiness, chewiness, and gumminess of zein-based cheese are shown in Fig. 4. 4 °C, 37 °C, and 60 °C were selected for textural analysis, respectively, because the texture profiles of cheese varied at different temperatures. The hardness, gumminess, and chewiness of all samples decreased with increasing temperature, which was attributed to the melting of solid fats and the softening of casein or zein networks at higher temperatures (Mattice & Marangoni, 2020b). The springiness of plant-based cheese remained relatively unchanged compared to Cheddar cheese with increasing temperature, except for Violife cheese, which increased by about four times at 60 °C. The protein content, types of starch, and synergistic interactions among ingredients were likely responsible for this observation (Grasso et al., 2021; Mattice & Marangoni, 2020b). The increased springiness of Vilofe cheese could be due to the viscoelasticity of its high

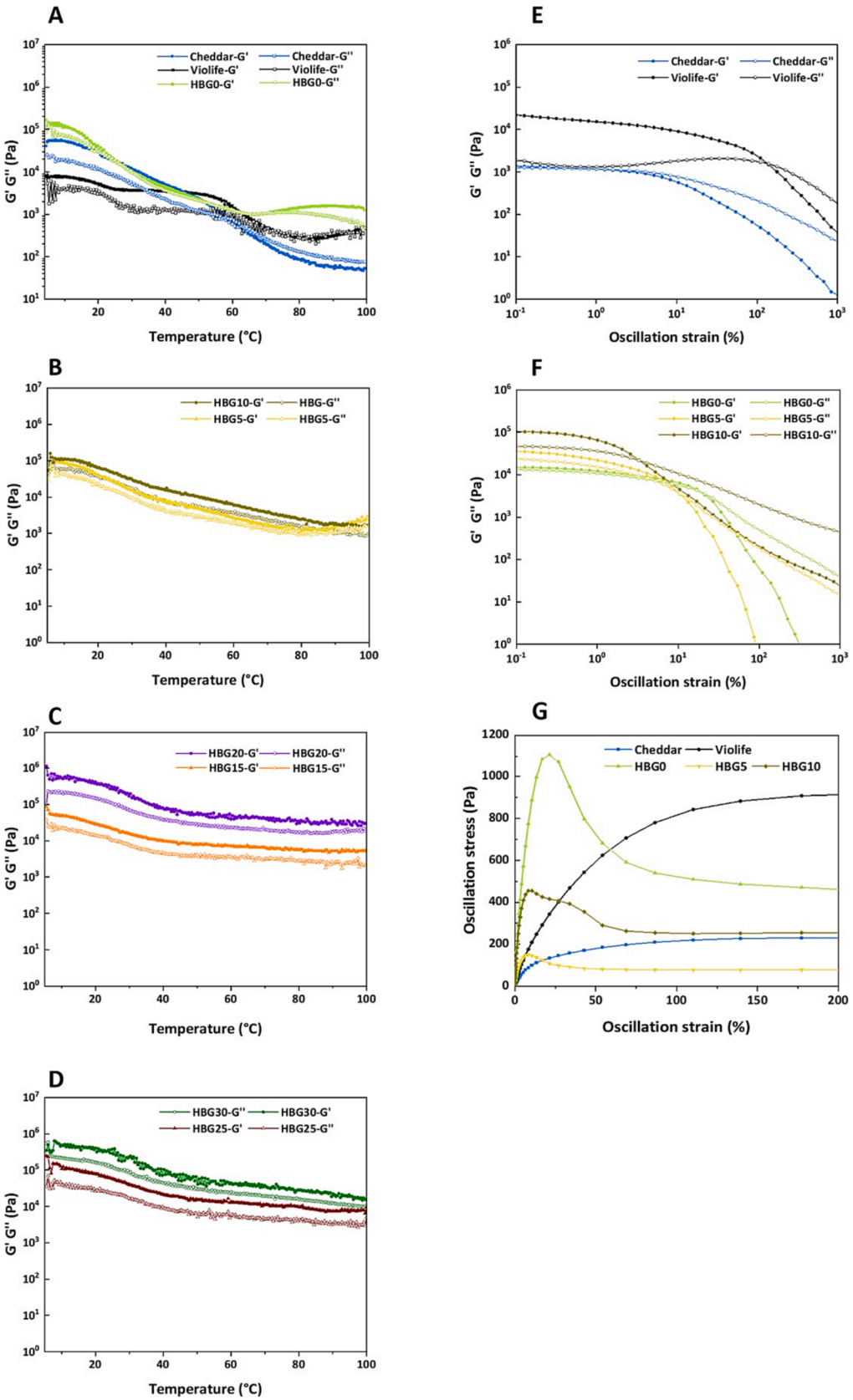

Fig. 3. Oscillatory temperature sweeps (A-D), oscillatory amplitude sweeps (E & F), and strain–stress curves (G) of Cheddar, Violife, and zein-based cheeses with different concentrations of highland barley β-glucan. HBG0, zein-based cheese without highland barley β-glucan; HBG5, zein-based cheese added with 5% highland barley β-glucan; HBG10, zein-based cheese added with 10% highland barley β-glucan; HBG15, zein-based cheese added with 15% highland barley β-glucan; HBG20, zein-based cheese added with 20% highland barley β-glucan; HBG25, zein-based cheese added with 25% highland barley β-glucan; HBG30, zein-based cheese added with 30% highland barley β-glucan.

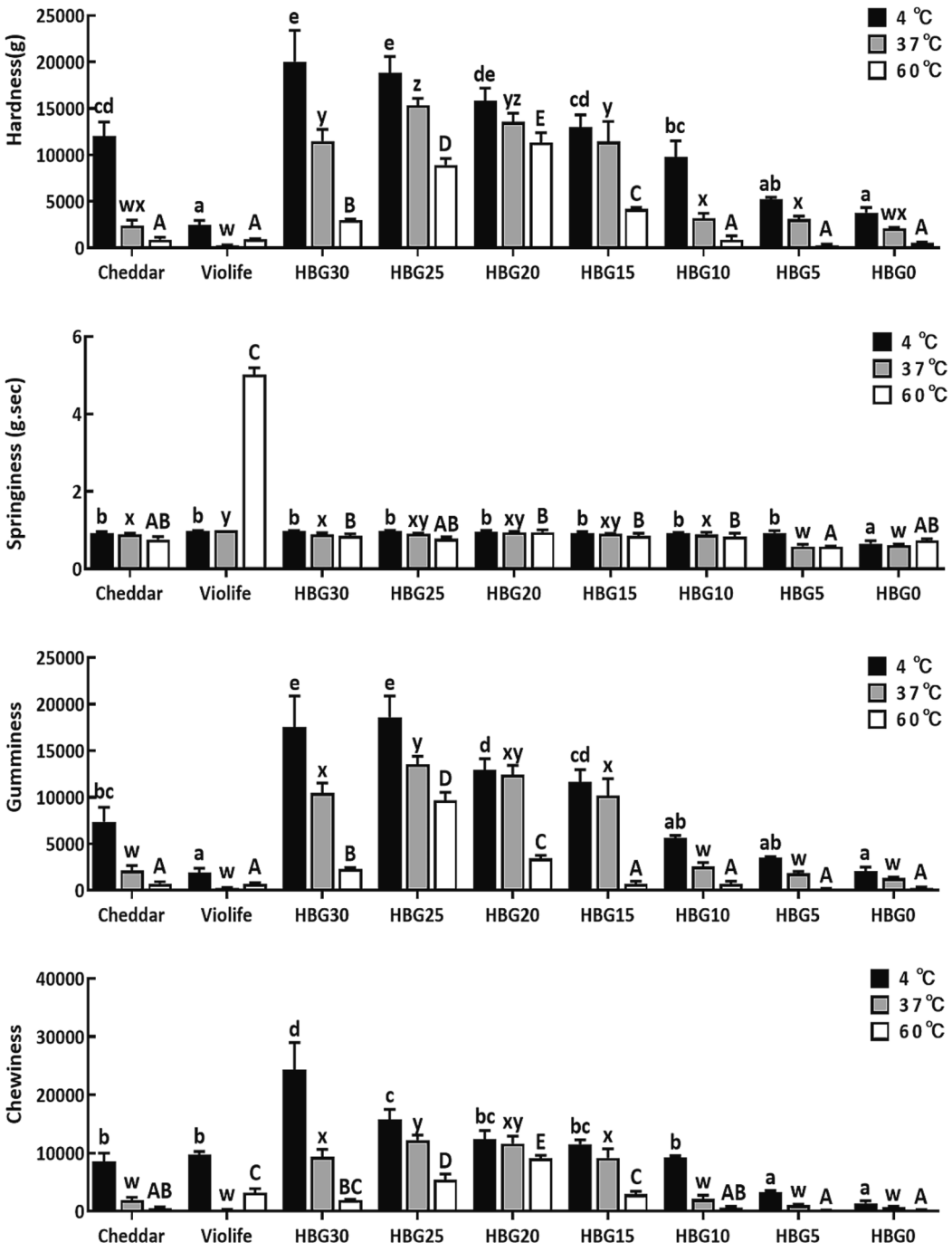

Fig. 4. Texture profile parameters at 4 °C, 37 °C and 60 °C of Cheddar, Violife, and zein-based cheeses with different concentrations of highland barley β-glucan. HBG0, zein-based cheese without highland barley β-glucan; HBG5, zein-based cheese added with 5 % highland barley β-glucan; HBG10, zein-based cheese added with 10 % highland barley β-glucan; HBG15, zein-based cheese added with 15 % highland barley β-glucan; HBG20, zein-based cheese added with 20 % highland barley β-glucan; HBG25, zein-based cheese added with 25 % highland barley β-glucan; HBG30, zein-based cheese added with 30 % highland barley β-glucan. Bars with different letters indicate statistically different ($p < 0.05$), where 4 °C samples (a-e), 37 °C (w-z) and 60 °C (A-E) analyzed separately.

starch content upon gelation at 60 °C (Mattice & Marangoni, 2020b). Our results showed at 4 °C, 37 °C, and 60 °C, Violife cheese lacked hardness and gumminess compared to Cheddar cheese. However, more similarities in hardness, springiness, chewiness, and gumminess were observed between HBG10 and Cheddar cheese. This was consistent with results reported by Volikakis et al, who found fortified 0.7 % β-glucan in low fat white-brined cheese exhibited similar hardness and firmness values to those of full-fat cheese (Volikakis et al., 2004).

4. Conclusion

In this study, zein-based plant cheese was constructed with different concentrations of HBG (0–30 %). Increasing HBG concentration led to smaller and more uniform oil droplets. FTIR analysis showed zein-HBG network created a 3D network via stretching intramolecular or intermolecular hydrogen bonds. The addition of HBG to zein resulted in a red shift in the UV absorption curve and an increased peak intensity at 280 nm. The SAXS pattern showed the scattering peak of HBG-zein based cheese was 0.603–0.895 nm^{-1} and R_g decreased from 0.963 nm to 0.567

nm as the concentration of HBG increased. The stretchability and free oil release of HBG-zein based cheese were more closely resembled those of Cheddar cheese than commercial Violife cheese. Specially, HBG10 was more comparable to Cheddar cheese in terms of rheological and textural properties. Our results emphasized the fact that plant-based cheese in the current market may lack critical cheese-like characteristics, and more efforts are needed to fill this gap using zein-based cheese. This study opens up significant opportunities for the creation of meltable low-fat plant-based cheese enriched with dietary fiber.

CRediT authorship contribution statement

Lijun Liu: Investigation, Writing – original draft, Visualization. **Guobao Huang:** Conceptualization, Funding acquisition, Resources. **Shuying Li:** Investigation. **Qifan Meng:** Investigation. **Fayin Ye:** Conceptualization, Writing – review & editing, Resources. **Jia Chen:** Conceptualization, Resources. **Jian Ming:** Conceptualization, Resources. **Guohua Zhao:** Conceptualization, Resources. **Lin Lei:** Conceptualization, Writing – review & editing, Funding acquisition, Supervision.

Declaration of Competing Interest

The authors declare that they have no known competing financial interests or personal relationships that could have appeared to influence the work reported in this paper.

Data availability

Data will be made available on request.

Acknowledgements

This work was supported by the Natural Science Foundation of Chongqing [grant number cstc2021jcyj-msxmX1097]; the Open Project Program of Guangxi Key Lab of Agricultural Resources Chemistry and Biotechnology [grant number 2021KF06]; the Chongqing Innovation and Human Capital Development Project for Returned Overseas Chinese; the Chongqing Technology Innovation and Application Development Project [grant number CSTB2022TIAD-KPX0092]; the National Key Research and Development Plan [grant number 2021YFD2100101]; and the Chongqing graduate research innovation project [grant number CYS22219]. The authors thank 1W2A SAXS station at the Beijing Synchrotron Radiation Facility (BSRF) for courteously supporting the SAXS analysis.

Appendix A. Supplementary data

Supplementary data to this article can be found online at https://doi.org/10.1016/j.fochx.2023.100907.

References

U.S. Retail Sales Data for the Plant-Based Foods Industry. (2021). *Plant Based Foods Association*. Available at: https://www.plantbasedfoods.org/2021-u-s-retail-sales-data-for-the-plant-based-foods-industry/.

Andersson, H., Öhgren, C., Johansson, D., Kniola, M., & Stading, M. (2011). Extensional flow, viscoelasticity and baking performance of gluten-free zein-starch doughs supplemented with hydrocolloids. *Food Hydrocolloids, 25*(6), 1587–1595. https://doi.org/10.1016/j.foodhyd.2010.11.028

Arifin, N. A. M., Mahamod, W. R. W., Bakar, N. A., Hashim, N., Isnolamran, N. H., & Shamsudin, S. A. (2021). The effect of virgin coconut oil content on the rheological profile of virgin coconut oil-based lamellar liquid crystal of mixed Tween 80: BRIJ 30 System. *Malaysian Journal of Microscopy, 17*, 13.

Arita-Merino, N., te Nijenhuis, L., van Valenberg, H., & Scholten, E. (2022). Multiple phase transitions and microstructural rearrangements shape milk fat crystal networks. *Journal of Colloid and Interface Science, 607*, 1050–1060. https://doi.org/10.1016/j.jcis.2021.09.071

Bai, Y.-P., Zhou, H.-M., Zhu, K.-R., & Li, Q. (2021). Effect of thermal processing on the molecular, structural, and antioxidant characteristics of highland barley β-glucan. *Carbohydrate Polymers, 271*, Article 118416. https://doi.org/10.1016/j.carbpol.2021.118416

Chalal, M., Ehrburger-Dolle, F., Morfin, I., Bley, F., Aguilar de Armas, M.-R., López Donaire, M.-L., … Casalegno, R. (2010). SAXS Investigation of the Effect of Temperature on the Multiscale Structure of a Macroporous Poly(N -isopropylacrylamide) Gel. *Macromolecules, 43*(4), 2009–2017. https://doi.org/10.1021/ma902655h

Chen, G., Dong, S., Chen, Y., Gao, Y., Zhang, Z., Li, S., & Chen, Y. (2020). Complex coacervation of zein-chitosan via atmospheric cold plasma treatment: Improvement of encapsulation efficiency and dispersion stability. *Food Hydrocolloids, 107*, Article 105943. https://doi.org/10.1016/j.foodhyd.2020.105943

Dai, S., Jiang, F., Shah, N. P., & Corke, H. (2019). Functional and pizza bake properties of Mozzarella cheese made with konjac glucomannan as a fat replacer. *Food Hydrocolloids, 92*, 125–134. https://doi.org/10.1016/j.foodhyd.2019.01.045

Erni, P., Windhab, E. J., Gunde, R., Graber, M., Pfister, B., Parker, A., & Fischer, P. (2007). Interfacial Rheology of Surface-Active Biopolymers: *Acacia senegal* Gum versus Hydrophobically Modifed Starch. *Biomacromolecules, 8*(11), 3458–3466. https://doi.org/10.1021/bm700578z

Florczuk, A., Załęcki, M., & Aljewicz, M. (2023). The applicability of Calcofluor White (CWS) and Fluorescent Brightener (CFB) dyes for confocal laser microscopic analysis (CLSM) of various β-glucans in selected dairy products and water. *Food Chemistry, 404*, Article 134508. https://doi.org/10.1016/j.foodchem.2022.134508

Fox, P. F., Guinee, T. P., Cogan, T. M., & McSweeney, P. L. H. (2017). Fundamentals of Cheese Science. *Springer, US.*. https://doi.org/10.1007/978-1-4899-7681-9

Grasso, N., Roos, Y. H., Crowley, S. V., Arendt, E. K., & O'Mahony, J. A. (2021). Composition and physicochemical properties of commercial plant-based block-style products as alternatives to cheese. *Future Foods, 4*, Article 100048. https://doi.org/10.1016/j.fufo.2021.100048

Grossmann, L., & McClements, D. J. (2021). The science of plant-based foods: Approaches to create nutritious and sustainable plant-based cheese analogs. *Trends in Food Science & Technology, 118*, 207–229. https://doi.org/10.1016/j.tifs.2021.10.004

Jin, B. (2020). Investigating on the interaction behavior of soy protein hydrolysates/β-glucan/ferulic acid ternary complexes under high-technology in the food processing: High pressure homogenization versus microwave treatment. *International Journal of Biological Macromolecules, 8*.

Khorshidian, N., Yousefi, M., Shadnoush, M., & Mortazavian, A. M. (2018). An Overview of β-Glucan Functionality in Dairy Products. *Current Nutrition & Food Science, 14*(4), 280–292. https://doi.org/10.2174/1573401313666170609092748

Kong, F., An, Y., Jiang, L., Tian, J., Yang, M., Li, M., … Yue, X. (2021). Spectroscopic and docking studies of the interaction mechanisms of xylitol with α-casein and κ-casein. *Colloids and Surfaces B: Biointerfaces, 206*, Article 111930. https://doi.org/10.1016/j.colsurfb.2021.111930

Konuklar, G., Inglett, G. E., Warner, K., & Carriere, C. J. (2004). Use of a β-glucan hydrocolloidal suspension in the manufacture of low-fat Cheddar cheeses: Textural properties by instrumental methods and sensory panels. *Food Hydrocolloids, 18*(4), 535–545. https://doi.org/10.1016/j.foodhyd.2003.08.010

Lamichhane, P., Kelly, A. L., & Sheehan, J. J. (2018). Symposium review: Structure-function relationships in cheese. *Journal of Dairy Science, 101*(3), 2692–2709. https://doi.org/10.3168/jds.2017-13386

Lilbæk, H. M., Broe, M. L., Høier, E., Fatum, T. M., Ipsen, R., & Sørensen, N. K. (2006). Improving the Yield of Mozzarella Cheese by Phospholipase Treatment of Milk. *Journal of Dairy Science, 89*(11), 4114–4125. https://doi.org/10.3168/jds.S0022-0302(06)72457-2

Liu, Y., Chen, L., Xu, H., Liang, Y., & Zheng, B. (2019). Understanding the digestibility of rice starch-gallic acid complexes formed by high pressure homogenization. *International Journal of Biological Macromolecules, 134*, 856–863. https://doi.org/10.1016/j.ijbiomac.2019.05.083

Ma, Y., Ye, F., Chen, J., Ming, J., Zhou, C., Zhao, G., & Lei, L. (2023). The microstructure and gel properties of linseed oil and soy protein isolate based-oleogel constructed with highland barley β-glucan and its application in luncheon meat. *Food Hydrocolloids, 140*, Article 108666. https://doi.org/10.1016/j.foodhyd.2023.108666

Mattice, K. D., & Marangoni, A. G. (2020a). Evaluating the use of zein in structuring plant-based products. *Current Research in Food Science, 3*, 59–66. https://doi.org/10.1016/j.crfs.2020.03.004

Mattice, K. D., & Marangoni, A. G. (2020b). Physical properties of plant-based cheese products with zein. *Food Hydrocolloids, 105*, Article 105746. https://doi.org/10.1016/j.foodhyd.2020.105746

McClements, D. J., & Grossmann, L. (2022). Next-Generation Plant-based Foods: Design, Production, and Properties. *Springer International Publishing*. https://doi.org/10.1007/978-3-030-96764-2

Moghiseh, N., Arianfar, A., Salehi, E. A., & Rafe, A. (2021). Effect of inulin/kefiran mixture on the rheological and structural properties of mozzarella cheese. *International Journal of Biological Macromolecules, 191*, 1079–1086. https://doi.org/10.1016/j.ijbiomac.2021.09.154

Muliawan, E. B. (2008). *Rheology and processing of mozzarella cheese* [University of British Columbia]. 10.14288/1.0058597.

Nicolás Saraco, M., & Blaxland, J. (2020). Dairy-free imitation cheese: Is further development required? *British Food Journal, 122*(12), 3727–3740. https://doi.org/10.1108/BFJ-11-2019-0825

Qiao, D., Tu, W., Wang, Z., Yu, L., Zhang, B., Bao, X., … Lin, Q. (2019). Influence of crosslinker amount on the microstructure and properties of starch-based superabsorbent polymers by one-step preparation at high starch concentration. *International Journal of Biological Macromolecules, 129*, 679–685. https://doi.org/10.1016/j.ijbiomac.2019.02.019

Rudan, M. A., & Barbano, D. M. (1998). A Model of Mozzarella Cheese Melting and Browning During Pizza Baking. *Journal of Dairy Science, 81*(8), 2312–2319. https://doi.org/10.3168/jds.S0022-0302(98)75812-6

Schober, T. J., Bean, S. R., Boyle, D. L., & Park, S.-H. (2008). Improved viscoelastic zein–starch doughs for leavened gluten-free breads: Their rheology and microstructure. *Journal of Cereal Science, 48*(3), 755–767. https://doi.org/10.1016/j.jcs.2008.04.004

Subramanian, A., Alvarez, V. B., Harper, W. J., & Rodriguez-Saona, L. E. (2011). Monitoring amino acids, organic acids, and ripening changes in Cheddar cheese using Fourier-transform infrared spectroscopy. *International Dairy Journal, 21*(6), 434–440. https://doi.org/10.1016/j.idairyj.2010.12.012

Sun, C., Dai, L., He, X., Liu, F., Yuan, F., & Gao, Y. (2016). Effect of heat treatment on physical, structural, thermal and morphological characteristics of zein in ethanol-water solution. *Food Hydrocolloids, 58*, 11–19. https://doi.org/10.1016/j.foodhyd.2016.02.014

Suzuki, T., Chiba, A., & Yarno, T. (1997). Interpretation of small angle x-ray scattering from starch on the basis of fractals. *Carbohydrate Polymers, 34*(4), 357–363. https://doi.org/10.1016/S0144-8617(97)00170-7

Volikakis, P., Biliaderis, C. G., Vamvakas, C., & Zerfiridis, G. K. (2004). Effects of a commercial oat-β-glucan concentrate on the chemical, physico-chemical and sensory attributes of a low-fat white-brined cheese product. *Food Research International, 37*(1), 83–94. https://doi.org/10.1016/j.foodres.2003.07.007

Wang, Y., Filho, F. L., Geil, P., & Padua, G. W. (2005). Effects of Processing on the Structure of Zein/Oleic Acid Films Investigated by X-Ray Diffraction. *Macromolecular Bioscience, 5*(12), 1200–1208. https://doi.org/10.1002/mabi.200500140

Ye, A., Hewitt, S., & Taylor, S. (2009). Characteristics of rennet–casein-based model processed cheese containing maize starch: Rheological properties, meltabilities and microstructures. *Food Hydrocolloids, 23*(4), 1220–1227. https://doi.org/10.1016/j.foodhyd.2008.08.016

Zhang, X., Gao, M., Zhang, Y., Dong, C., Xu, M., Hu, Y., & Luan, G. (2022). Effect of plasticizer and zein subunit on rheology and texture of zein network. *Food Hydrocolloids, 123*, Article 107140. https://doi.org/10.1016/j.foodhyd.2021.107140

Zhang, Y., Chen, C., Chen, Y., & Chen, Y. (2019). Effect of rice protein on the water mobility, water migration and microstructure of rice starch during retrogradation. *Food Hydrocolloids, 91*, 136–142. https://doi.org/10.1016/j.foodhyd.2019.01.015

Zhang, Y., Junejo, S. A., Zhang, B., Fu, X., & Huang, Q. (2022). Multi-scale structures and physicochemical properties of waxy starches from different botanical origins. *International Journal of Biological Macromolecules, 220*, 692–702. https://doi.org/10.1016/j.ijbiomac.2022.08.133

Zhang, Y., Xu, M., Zhang, X., Hu, Y., & Luan, G. (2022). Application of zein in gluten-free foods: A comprehensive review. *Food Research International, 160*, Article 111722. https://doi.org/10.1016/j.foodres.2022.111722